

Electrical characterizations of SnPc/*p*-GaAs heterojunction

M.M. El-Nahass^{1,a} and A.S. Faidah²

¹ Physics department, Faculty of Education, Ain Shams University, Roxy 11757, Cairo, Egypt

² Physics Department, Faculty of Science, King Abdul Aziz University, Jeddah, Saudi Arabia

Received: 2 August 2008 / Received in final form: 31 December 2008 / Accepted: 15 January 2009
Published online: 8 April 2009 – © EDP Sciences

Abstract. Current voltage and capacitance-voltage characteristics for SnPc thin film with ~ 105 nm thickness; deposited on *p*-GaAs single crystals have been investigated. The dark current voltage-characteristics of the prepared junction have been investigated in a temperature range from ~ 303 to 393 K. The obtained results showed rectification behaviour. At low forward and reverse bias, the current was found to be limited by the thermoionic emission, while at high forward voltage, space charge limited current dominated by a single trap level of 0.22 eV. The analysis of the dark capacitance voltage characteristics indicated that the carrier concentration is $1.4 \times 10^{14} \text{ cm}^{-3}$ with a built in voltage ~ 0.55 eV.

PACS. 81.15.Fg Laser deposition – 73.40.-c Electronic transport in interface structures – 73.50.Pz Photoconduction and photovoltaic effects

1 Introduction

In the last few decades, the organic semiconductors have a great attention as promising materials for future technological devices due to their function and variety. Among these organic materials are the phthalocyanines, which are prototype organic semiconductors. These Pcs' which characterized by high thermal and chemical stability. They form large group of organic compounds, which have been the main basis for the search of molecular semiconductors for more than 40 years. Therefore, numerous searches have been done for phthalocyanines mainly in thin films form. Despite that they have been studied since 1930 [1], the interest in their properties is still attractive because of their potential applications as semiconducting devices such as photovoltaic cells [2] laser printers [3], dyes, pigments, photocopying agents [4] gas sensors [5,6], optical data storage systems [7], solar cells [8], light emitting diodes [9] and also in nuclear reactor systems [10]. Despite that most of the organic photovoltaic cells have been fabricated with low efficiencies [11–14], a significant jump in the conversion yield of organic photovoltaic (PV) solar cells, took place passing from 1% yield [15] to about 5% [16].

Some efforts were done on the fabrication of photovoltaic devices based on SnPc demonstrated by Yang et al. [17]. They also described an organic photovoltaic cell based on a tin II phthalocyanine SnPc/C₆₀ donor/acceptor heterojunction with sensitivity at wavelengths of 900 nm. They found that the obtained low

hole mobility in polycrystalline thin films of SnPc, led to low fill factors and therefore low-power conversion efficiencies. However, owing to its large absorption coefficient, a 50 Å thick layer of SnPc yields solar cell external quantum efficiencies of up to 21% at 750 nm. With the double heterostructure of indium-tin oxide/100 Å copper phthalocyanine (50 Å)/SnPc (540 Å)/C₆₀(75 Å) bathocuproine/Ag. They have obtained a power conversion efficiency of $1.0 \pm 0.1\%$ under 1 sun standard AM1.5G solar illumination and efficiencies of $1.3 \pm 0.1\%$ under intense (10 suns) standard AM1.5G solar illumination. Rand et al. [18] have demonstrated an optimized copper phthalocyanine CuPc/SnPc/C₆₀ nanocrystalline network and then they obtained a power conversion efficiency of $2.90 \pm 0.2\%$ under 100 mW/cm², AM1.5G illumination. They found that the open circuit voltage of the simultaneous heterojunction is determined by the lowest voltage of the separate donor/acceptor constituent junctions.

In the present work, Au/SnPc/*p*-GaAs/Al as a heterojunction was fabricated by deposition of SnPc thin films using the thermal evaporation technique onto *p*-GaAs single crystals. The temperature dependence of the current-voltage (*I*-*V*) characteristics in both forward and reverse bias was studied in a temperature range (~ 303 –393 K) and in a voltage range extended from -1.6 to $+1.6$ V, to obtain information about the transport mechanisms of the device. In addition, capacitance voltage (*C*-*V*) measurements were applied for these heterojunction to obtain information about the carrier concentration and the built in voltage.

^a e-mail: prof_nahhas@yahoo.com

2 Experimental details

The SnPc powder used in this study was obtained from Kodak, UK. The *p*-type GaAs single crystal wafer with carrier concentration of $1.5 \times 10^{17} \text{ m}^{-3}$ was obtained from Sparta chemical industries, New Jersey, USA Co. A piece of $50.8 \times 45 \text{ mm}$ and (100) orient, was cleaned and etched. After etching, the GaAs wafer was washed with distilled water and then with ethylalcohol. Then the GaAs wafer was coated from the front side by SnPc thin film of 105 nm thicknesses using the conventional thermal evaporation technique, and then the SnPc layer was overcoated by an Au mesh to be used as ohmic electrode. The back side of the GaAs was coated by a thick layer of aluminium electrode. It was found that the annealing of the fabricated junction at 100 K for one hour is needed to enhance the performance of the junction. This annealing might remove any channels, which could be raised during the fabrication. Measurement of the dark current-voltage characteristics within the temperature range 303 to 393 K were made in air. The current flowing through the cell from a stabilized power supply was determined by using Keithley 617 electrometer. The temperature was measured directly by mean of Pt-PtRh thermocouple with monitor (Philips thermostat PT 22S2 A). A proportional temperature controller was used to avoid the sudden drop in the heater temperature. The dark *C-V* characteristics were measured at 1 MHz by using a model 410 CV meter.

3 Results and discussion

3.1 Dark current-voltage characteristics

To study the junction properties, current-voltage characteristics (*J-V*) have been made. These measurements, usually, provide a valuable source of information about the junction properties such as the rectification ratio (*RR*), the diode quality factor (*m*), the saturation current density (J_0), the series (R_s) and the shunt (R_{sh}) resistances. Analysis of the *J-V* characteristics is also extremely useful to identify the transport mechanisms controlling the conduction. *J-V* characteristics of SnPc film with thickness $\sim 105 \text{ nm}$ deposited onto *p*-GaAs at different temperatures ranging from 303 to 393 K are illustrated in Figure 1. The curves exhibited a diode-like behaviour, with the forward direction in the positive potential on GaAs. The observed exponential dependence at lower voltage range can be attributed to the formation of depletion region between GaAs and SnPc thin Film.

From this figure, the junction parameters can be easily determined. For applied voltage $> 0.7 \text{ V}$, the curves deviated from the exponential behavior due to the effect of the series resistance (R_s) and the shunt resistance (R_{sh}). The *J-V-T* characteristics could be described, in the forward direction, by modified Shockley equation;

$$J = J_0 \{ \exp(q(V - IR_s)/mk_B T) - 1 \} + (V - IR_s)/R_{sh} \quad (1)$$

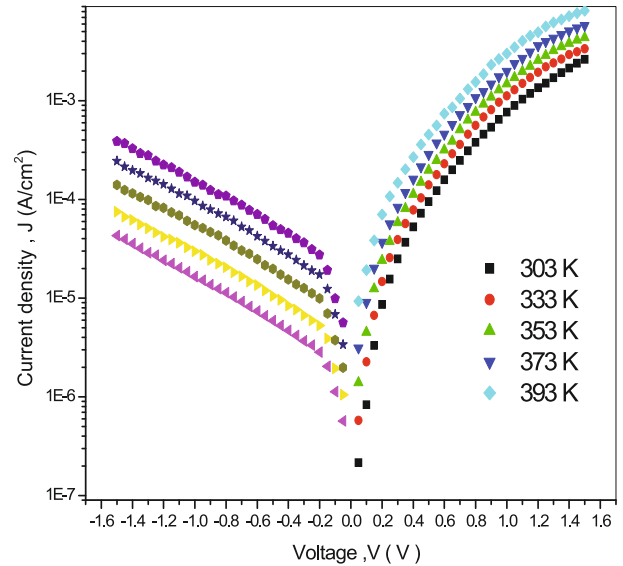


Fig. 1. (Color online) *J-V* characteristics of SnPc/*p*-GaAs heterojunction at different temperatures in both forward and reverse bias.

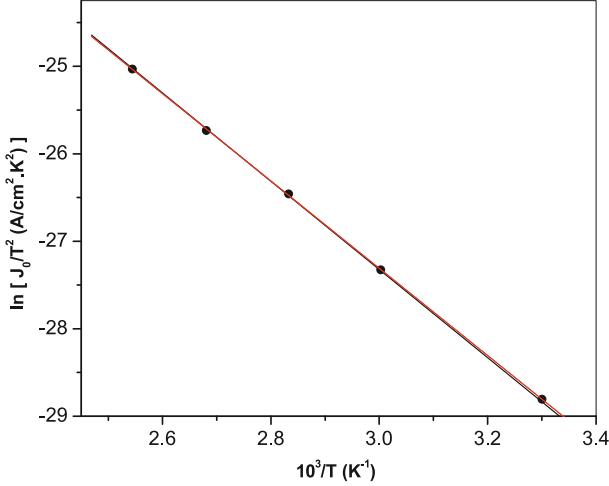
where *m* is the ideality factor, k_B is Boltzmann's Constant, J_0 is the saturation current density, *T* is the absolute temperature, *q* is the electronic charge carrier. Since the rectification ratio (*RR*) for the junction is defined as the ratio of the forward current to the reverse current density at a certain value of the applied voltage, i.e. $RR = (J_f/J_r)_{v=const.}$, the calculated values of *RR* for the prepared heterojunction (Hj) at a voltage value $\sim 1 \text{ V}$ is equal to 58.6. Since the junction resistance (R_j) = $(\delta V/\delta I)_{T=const.}$, it could be determined from the dark *J-V* curves. For sufficiently high forward biasing the junction resistance approached a constant value. This value is the series resistance (R_s). For sufficiently high reverse biasing, the junction resistance was also constant, which is equal to the diode shunt resistance R_{sh} due to the leakage current through the junction. The obtained values, for R_{sh} and R_s at room temperature ($\sim 300 \text{ K}$) are $0.3 \text{ M}\Omega$ and $4.3 \text{ K}\Omega$, respectively. The decrease in R_{sh} by increasing the applied voltage and the departure from the ideality may be due to the surface effects on *p-n* junctions. Figure 2 shows two regions with different slopes indicating the presence of two types of conduction mechanisms which depends strongly on the slope. These behaviours could be represented by the following formula [19];

$$J = J_{01} [\exp(q(V - IR_s)/m_1 k_B T) - 1] + J_{02} [(\exp(q(V - IR_s)/m_2 k_B T) - 1) + [(V - IR_s)/R_{sh}]. \quad (2)$$

All the symbols included in the above equation have the same meaning as in equation (1), each region was analyzed separately to determine the predominant conduction mechanism for the Au/SnPc/GaAs/Al cell. This aim included four steps; (1) determination and analysis of the values of the ideality factor and its dependence on the temperature; (2) the analysis of the bucking current vs. the

Table 1. The values of saturation current density J_0 and ideality factor m .

T (K)	m_1	J_{01} (A/cm ²)	m_2	J_{02} (A/cm ²)
303	1.54	6.7×10^{-8}	7.84	8.9×10^{-6}
333	1.61	1.96×10^{-7}	7.11	1.2×10^{-5}
353	1.71	6.36×10^{-7}	6.87	1.75×10^{-5}
373	1.9	1.6×10^{-6}	6.6	2.5×10^{-5}
393	2.19	5.2×10^{-6}	6.8	4.1×10^{-5}


Fig. 2. (Color online) Semilogarithmic plot of $\ln(J_0/T^2)$ versus $10^3/T$ for SnPc/p-GaAs heterojunction.

applied voltage at constant temperature; (3) the analysis of the bucking current versus the temperature at constant voltage, and finally; (4) the analysis of the saturation current to explore the predominant conduction mechanism. In the first region the parameters J_{01} and m_1 were determined by a reasonable fitting of the curves lower than 0.25 V, and the values of J_{01} and m_1 were determined and listed in Table 1. It is clear from this table that in this voltage region the junctions showed that $1 > m_1 > 2$, which may be attributed to the recombination of electrons and holes in the depletion region, and also to the increased effect of the diffusion current on increasing of the applied voltage [19]. The reverse saturated current (J_{01}), see Figure 2, could be represented by the following relation:

$$(J_{01})/T^2 \approx A^* A [\exp(-\Phi_b/m_1 K_B T)] \quad (3)$$

where Φ_b is the potential barrier height, A is the area of the cell and A^* is the Richardson constant. The obtained data indicate that the predominant mechanism in this voltage region < 0.25 V is the thermoionic emission. The second region, which deals with voltage > 0.25 V up to $V \geq 0.8$, was analyzed. The values of the ideality factor are very greater than two. It may be due to the representation of space charge limited current SCLC. To deduced that J - V - T characteristics were re-plotted on logarithmic scale, see Figure 3, where a quadratic dependence of current on voltage ($J \propto V^2$) over the potential range (~ 0.2 – 0.8 V)

was observed. Such a power dependence suggest that the current is a space-charge-limited current (SCLC). The current in this case is expressed by:

$$J = (9/8)\varepsilon\mu(V^2/d^3)(N_V/N_t) \exp(-E_t/K_B T) \quad (4)$$

where ε is the permittivity of p -SnPc which is taken as 2.42×10^{-11} Fm⁻¹, $\mu \sim 10^{-4}$ cm²/Vs and $N_V \sim 10^{27}$ /cm³ [20] and N_t is the concentration of traps at energy level E_t , above the valence band edge calculated as 5.46×10^{18} /cm³ and 0.22 eV at room temperature ~ 303 K, respectively.

The reverse J - V characteristics of SnPc/p-GaAs were analyses at room temperature (Fig. 4), in the form of $\ln J_r$ vs. $V^{1/2}$ at constant temperature, and clearly yield two distinct regions with different slopes which may be interpreted in terms of either Schottky (field-lowering of interfacial barrier at the injecting electrode interface) or Poole-Frenkel (field-assisted thermal detrapping of carriers) effect. The I - V expressions for these processes are given for the Schottky effect and for the Poole-Frenkel effect, respectively, by [21]:

$$\begin{aligned} J &= A^{**} T^2 \exp(-\varphi_s/k_B T) \exp(\beta_s V^{1/2}/k_B T d^{1/2}) \\ J &= J_0 \exp(\beta_{PF} V^{1/2}/k_B T d^{1/2}) \end{aligned} \quad (5)$$

where A^{**} is the effective Richardson constant, φ_s the Schottky barrier height at the injected electrode interface, J_0 the low-field current and β_s and β_{PF} are the Schottky and Poole-Frenkel field-lowering coefficients, respectively. The calculated values were of $\beta_s = 6.6 \times 10^{-5}$ eV m^{1/2} V^{-1/2} and $\beta_{PF} = 13.2 \times 10^{-5}$ eV m^{1/2} V^{-1/2} in the lower voltage range and $\beta_s = 3.09 \times 10^{-5}$ eV m^{1/2} V^{-1/2} and $\beta_{PF} = 6.18 \times 10^{-5}$ eV m^{1/2} V^{-1/2} in the higher voltage range. Similar behaviour has been reported previously for phthalocyanine films using aluminum-injected electrodes [21]. Using the theoretical value of β_s in equation (5), together with the slope and the intercept of lower-voltage region in Figure 4, the value of φ_s can be estimated and has the value 0.21 eV.

3.2 C-V characteristics

Figure 5 shows the C - V characteristics of the SnPc/p-GaAs heterojunction measured in dark at room temperature and at increment voltage of frequency 1 MHz. Taking into account the dielectric relaxation time, for both of GaAs and SnPc used in this study. It is found that the values of τ are of the order 10^{-11} and 10^{-6} s for GaAs and SnPc, respectively, suggesting that the redistribution of free carrier inside the GaAs side can respond to the frequency of 1 MHz while that of SnPc cannot. From this point of view can be obtain information about the depletion region extending in the GaAs side regardless of that of SnPc side. The capacitance of the SnPc film is equal to its geometrical capacitance. Accordingly, the total capacitance of the device can be expressed by two series capacitors, one corresponds to

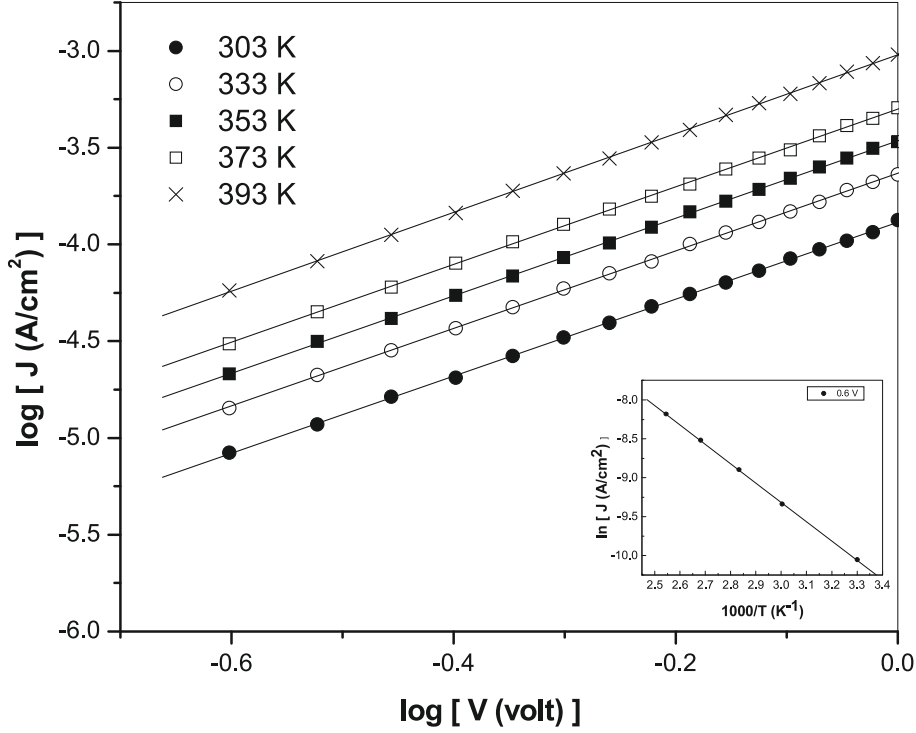


Fig. 3. Variation of $\log J$ with $\log V$ at higher forward voltage bias for SnPc/*p*-GaAs heterojunction and variation of $\log J$ with $1000/T$ in SCLC for SnPc/*p*-GaAs heterojunction.

the junction capacitance and the other to the geometrical capacitance. It is clear that C^{-2} increases linearly with increasing the reverse applied voltage indicating that the junction is a one-side abrupt junction. The relation between the junction capacitance, C and the reverse applied potential for an abrupt junction can be given by [22]:

$$\frac{1}{C^2} = -\frac{2}{eN\epsilon\epsilon_0}(V_b - V) \quad (6)$$

where V_{bi} is the built-in voltage, N is the free carrier concentration, A is the effective area (10^{-4} m^2) and ϵ is the dielectric constant. The carrier concentration can be estimated experimentally from the relation

$$\frac{d(C^{-2})}{dV} = -\frac{2}{e\epsilon\epsilon_0NA^2}. \quad (7)$$

The estimated carrier concentration is $1.4 \times 10^{14} \text{ cm}^{-3}$. The built-in potential was estimated from the intercept with the horizontal asymptote as 0.55 V.

3.3 Photovoltaic properties

The I - V characteristics of SnPc/*p*-GaAs heterojunction under illumination, measured at room temperature, are illustrated in Figure 6. The solar cell parameters for the heterojunction such as the open circuit voltage V_{oc} , short circuit current I_{sc} , were obtained to be 600 mV and $82 \mu\text{A}$, respectively. The fill factor FF, and the power conversion

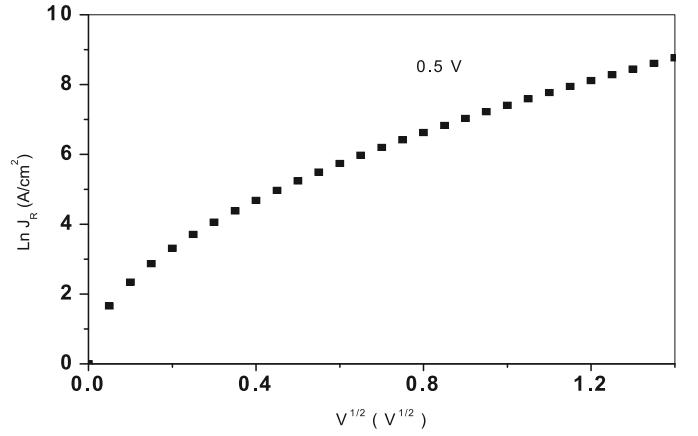


Fig. 4. Reverse J - V characteristics of SnPc/*p*-GaAs cell at room temperature.

efficiency η , as estimated given by:

$$FF = \frac{P_{max}}{V_{oc}I_{sc}} \quad (8)$$

where P_{max} is the maximum output power collected from the solar cell. From Figure 6 the values of the P_{max} and FF were 17.81 W/m^2 and 0.34, respectively. The obtained poor filling factor can be ascribed to the low shunt resistance value. The power conversion efficiency, is defined by the ratio of the maximum output power collected from a

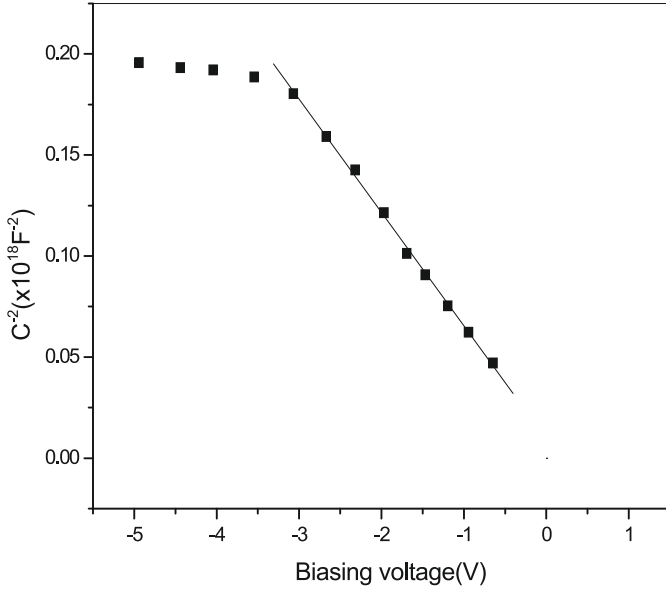


Fig. 5. $1/C^2$ - V characteristic for of SnPc/*p*-GaAs heterojunction.

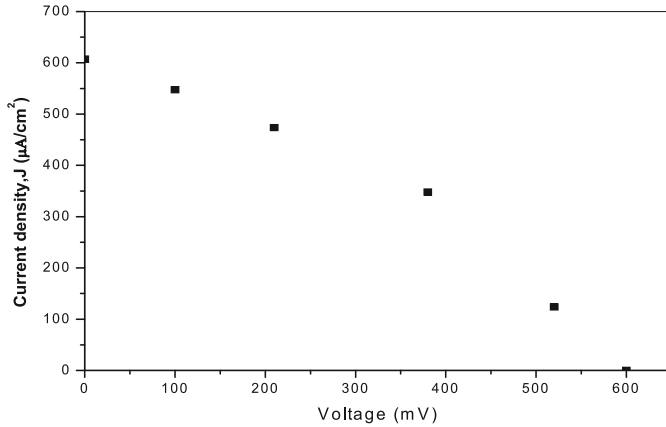


Fig. 6. Load J - V characteristics under 6 mW/cm^2 illumination for SnPc/*p*-GaAs cell.

solar cell to the input power of the incident light, P in and is given by [19]:

$$\eta = \frac{FFI_{sc}V_{oc}}{p_{in}} 100\%. \quad (9)$$

The value of η was estimated as 2.9% the obtained power conversion efficiency in this work reflects the good selection of materials constructing the device.

3.4 Spectral response

Figure 7 shows that the spectral response of V_{oc} , respectively of SnPc/*p*-GaAs solar cell matches the more energetic portion of the solar radiation ranging from 200 nm

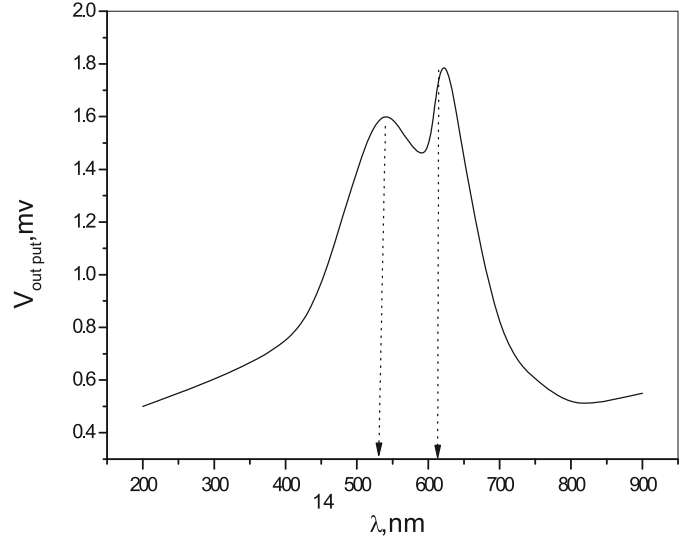


Fig. 7. Spectral response of SnPc/*p*-GaAs solar cell.

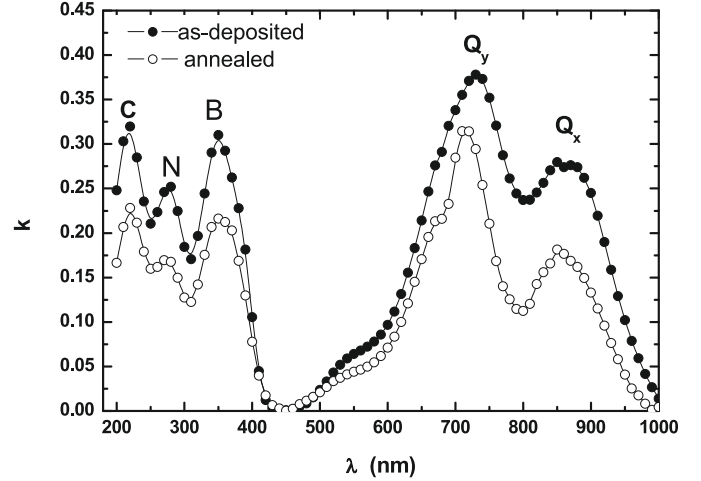


Fig. 8. The imaginary part of the index of refraction for SnPc film.

up to 1000 nm. The prepared cell showed a major response peak at about $0.55 \mu\text{m}$ and a second one at about $605 \mu\text{m/cm}^2$, which may be related to the optical absorption through SnPc at 2.25 eV and 2.05 eV. The reported results were made using an electrometer (Keithley 617). The action spectrum is similar to spectral dependence of the imaginary part of the index of refraction for SnPc (Fig. 8), which give support for the active region for the light effect lies in the SnPc layer.

4 Conclusions

The organic/inorganic heterojunctions were studied. The SnPc thin film with $\sim 105 \text{ nm}$ thickness; deposited on *p*-GaAs single crystals by evaporation technique. The current-voltage (I - V) and capacitance-voltage (C - V)

measurements have been performed to determine the electrical properties of the junctions. The junctions exhibit rectifying characteristics showing $p-p+$ diode-like behaviour. Measurements of the forward current versus voltage, and the saturation current versus inverse temperature.

The rectification ratio of the junction was also calculated at ± 1 V, yielding a value of 58.6. The dark.

Current-voltage measurements suggest that the forward current in these junctions involves thermionic emission mechanism, while at high-applied voltage a space-charge-limited current mechanism was operated. On the other hand, the reverse current may be two distinct regions with different slopes which may be interpreted in terms of either Schottky (field-lowering of interfacial barrier at the injecting electrode interface) or Poole-Frenkel (field-assisted thermal detrapping of carriers) effect. From the capacitance-voltage measurements at high frequency of 1 MHz, one can obtain information on the depletion layer. The $C-V$ measurements showed that the junction is of abrupt nature with built-in voltage of 0.55. Under illumination, the SnPc/ p -GaAs cell showed promising photovoltaic properties and had solar conversion efficiency of 2.9%.

References

1. R.P. Listead, J. Chem. Soc. Part I, 1016 (1934)
2. D. Wohrle, D. Meissner, Adv. Mater. **3**, 129 (1991)
3. P. Gregory, *High-technology Applications of Organic Colorants* (Plenum Press, New York, 1991), p. 759
4. P. Haisch, G. Winter, M. Hanack, L. Luer, H.J. Egelhaaf, D. Oelkrug, Adv. Mater. **9**, 316 (1997)
5. J.W. Gardner, M.Z. Iskandari, B. Bott, Sens. Actuat. B **9**, 133 (1992)
6. A. Mrwa, M. Friedrich, A. Hofmann, D.R.T. Zahn, Sens. Actuat. B: Chem. **24-25**, 596 (1995)
7. R. Ao, L. Kümmerl, D. Haarer, Adv. Mater. **7**, 495 (1995)
8. H.R. Kerp, E.E. Van Faassen, Chem. Phys. Lett. **332**, 5 (2000)
9. S.T. Lee, Y.M. Waug, X.Y. Hou, C.W. Tang, Appl. Phys. Lett. **74**, 670 (1999)
10. P. Cerny, Chem. Zvesti **9**, 94 (1955)
11. P.J. Reucroft, H. Ullal, Sol. Energy Mater. **2**, 217 (1979/1980)
12. A.K. Ghosh, D.L. More, T. Feug, R.F. Shaw, C.A. Rowe, J. Appl. Phys. **45**, 230 (1974)
13. M. Khelifi, M. Mejatty, J. Berrehar, H. Bouchrriha, Rev. Phys. Appl. **20**, 511 (1985)
14. A.K. Mahapatro, S. Ghosh, IEEE Trans. Electron. Dev. **48**, 1911 (2001)
15. C.W. Tang, Appl. Phys. Lett. **48**, 183 (1986)
16. J.H. Schön, Ch. Kloc, B. Batlogg, Appl. Phys. Lett. **77**, 2473 (2000)
17. F. Yang, R.R. Lunt, S.R. Forrest, Appl. Phys. Lett. **92**, 053310 (2008)
18. B.P. Rand, J. Xue, F. Yang, S.R. Forrest, Appl. Phys. Lett. **87**, 233508 (2005)
19. M.M. El-Nahass, K.F. Abd-El-Rahamann, A.A.M. Farag, A.A.A. Darwish, Organic. Electr. **3**, 129 (2005)
20. T.G. Abdel-Malik, R.M. Abdel-Latif, A.E. El-Samahy, S.M. Khalil, Thin Solid Films **256**, 139 (1995)
21. M.M. El-Nahass, K.F. Abd-El-Rahamann, J. Alloys Compds. **430**, 194 (2007)
22. E.H. Rhoderick, *Metal Semiconductor Contacts* (Oxford University Press, Oxford, 1978)